Space Weather

RESEARCH ARTICLE
10.1029/2024SW004213

On the Extraordinary L-Band Scintillation Event Observed in the American Sector During the 23–24 March 2023 Geomagnetic Storm

J. Gomez Socola[1], F. S. Rodrigues[1], J. Sousasantos[1], M. R. Quesada[2], R. Heelis[1], Y. Otsuka[3], A. Shinbori[3], M. Nishioka[4], and S. Perwitasari[4]

[1]The University of Texas at Dallas, Richardson, TX, USA, [2]Costa Rica Institute of Technology, Cartago, Costa Rica, [3]Institute for Space-Earth Environmental Research, Nagoya University, Nagoya, Japan, [4]National Institute of Information and Communications Technology, Tokyo, Japan

Abstract We report an extraordinary L-band scintillation event detected in the American sector on the night of 23–24 March 2023. The event was detected using observations distributed from the magnetic equator to mid latitudes. The observations were made by ionospheric scintillation and total electron content (TEC) monitors deployed at the Jicamarca Radio Observatory (JRO, ∼−1° dip latitude), at the Costa Rica Institute of Technology (CRT, ∼20° dip latitude), and at The University of Texas at Dallas (UTD, ∼42° dip latitude). The observations show intense pre- and post-midnight scintillations at JRO, a magnetic equatorial site where L-band scintillation is typically weak and limited to pre-midnight hours. The observations also show long-lasting extremely intense L-band scintillations detected by the CRT monitor. Additionally, the rare occurrence of intense mid-latitude scintillation was detected by the UTD monitor around local midnight. Understanding of the ionospheric conditions leading to scintillation was assisted by TEC and rate of change of TEC index (ROTI) maps. The maps showed that the observed scintillation event was caused by equatorial plasma bubble (EPB)-like ionospheric depletions reaching mid latitudes. TEC maps also showed the occurrence of an enhanced equatorial ionization anomaly throughout the night indicating the action of disturbance electric fields and creating conditions that favor the occurrence of severe scintillation. Additionally, the ROTI maps confirm the occurrence of pre- and post-midnight EPBs that can explain the long duration of low latitude scintillation. The observations describe the spatio-temporal variation and quantify the severity of the scintillation impact of EPB-like disturbances reaching mid latitudes.

Plain Language Summary Scintillation can be described as rapid fluctuations in the phase and/or amplitude of radio signals that propagate through the Earth's ionosphere such as those used by Global Positioning System (GPS) receivers. Scintillation is caused by ionospheric density perturbations and is known to impact the performance of systems used for communication, navigation and remote sensing. Scintillation events are commonly observed at low and high latitudes, but a reduced number of cases of scintillation at mid latitudes have been reported. Here, we present the case of an extremely intense and long-lasting scintillation event that extended from low to mid latitudes, observed on 23–24 March 2023. The event was captured by a network of ionospheric scintillation monitors recently developed and deployed in South America, Central America and US. In addition to reporting the occurrence of the extraordinary scintillation event, the space weather conditions associated with it are discussed.

Key Points:

- We report the occurrence of rare intense mid-latitude L-band scintillation in southern US during the geomagnetic storm of 23–24 March 2023
- The event was accompanied by severe scintillation at the equator and extremely severe and long-lasting scintillation at low latitudes
- The extraordinary scintillation event represents the space weather impact of an extreme EPB-like TEC disturbance on GNSS signals

Correspondence to:
J. Gomez Socola,
Josemaria.GomezSocola@UTDallas.edu

Citation:
Gomez Socola, J., Rodrigues, F. S., Sousasantos, J., Quesada, M. R., Heelis, R., Otsuka, Y., et al. (2025). On the extraordinary L-band scintillation event observed in the American sector during the 23–24 March 2023 geomagnetic storm. *Space Weather*, *23*, e2024SW004213. https://doi.org/10.1029/2024SW004213

Received 9 OCT 2024
Accepted 7 MAY 2025

Author Contributions:
Data curation: J. Gomez Socola, Y. Otsuka, A. Shinbori, M. Nishioka, S. Perwitasari
Formal analysis: J. Gomez Socola, F. S. Rodrigues, J. Sousasantos, R. Heelis
Funding acquisition: F. S. Rodrigues
Investigation: J. Gomez Socola
Methodology: J. Gomez Socola
Writing – original draft: J. Gomez Socola
Writing – review & editing: F. S. Rodrigues, J. Sousasantos, M. R. Quesada, R. Heelis, Y. Otsuka, A. Shinbori, M. Nishioka, S. Perwitasari

1. Introduction

Ionospheric scintillation is often cited as a critically important component of space weather. It is described as rapid fluctuations in the amplitude and/or phase of transionospheric radio signals (Kintner et al., 2007; Yeh & Liu, 1982). Scintillation is caused as a result of the diffraction and/or refraction of radio waves due to irregularities in the density of the Earth's ionospheric plasma.

Scintillation adversely affects the performance of civilian and military systems that rely on transionospheric signals for communication, navigation, and remote sensing (Bevis et al., 1994; Carrano et al., 2012; Kelly et al., 2014; Luo et al., 2023; Moraes et al., 2024; Sousasantos et al., 2021; Zakharenkova & Cherniak, 2021). Therefore, significant efforts have been directed toward developing and improving ionospheric models that

predict scintillation events (Basu et al., 1976; Groves et al., 1997; Kelley & Retterer, 2008; McGranaghan et al., 2018; Redmon et al., 2010; Veettil et al., 2018).

A large number of specialized monitors for studies of ionospheric scintillation have been deployed at low and high latitudes over the American sector, and an extensive number of studies have reported the properties of scintillation events as recorded by these monitors. For instance, the Low-latitude Ionospheric Sensor Network (LISN) provides observations of scintillation at low latitudes in the American sector (Valladares & Chau, 2012), typically associated with Equatorial Plasma Bubbles (EPBs). The INCT GNSS-NavAer network (a follow-on of the CIGALA/CALIBRA network) also contributes with low latitude measurements in South America (de Paula et al., 2023; Monico et al., 2013, 2022). The Canadian High Arctic Ionospheric Network (CHAIN) is another example of network designed to observe the ionospheric response to space weather events, but at high latitudes (Jayachandran et al., 2009). Deployment of network of scintillation monitors at low and high latitudes have been justified by an understanding that different types of ionospheric perturbations leading to scintillation-causing irregularities occur very often in these regions (Aarons, 1982; Jiao & Morton, 2015; Liu et al., 2012).

The mid-latitude region, on the other hand, has been thought, for a long time, to be devoid of significant ionospheric perturbations that could lead to irregularities and significant scintillation (Erickson, 2020; Hysell et al., 2018; Kintner et al., 2007). As a result, the deployment and operation of specialized ionospheric scintillation monitors at mid latitudes (e.g., United States of America) was difficult to justify, leading to a reduced number of appropriate observations in this region.

Ledvina et al. (2002) reported the first detection of intense Global Positioning System (GPS) scintillations at mid latitudes. The observations were made by a monitor operating in the northeastearn US (Ithaca–NY, 53.36° dip latitude) on 25–26 September 2001, and scintillation attributed to ionospheric irregularities associated with an equatorward movement of the ionospheric trough and a storm time-enhanced density (SED) disturbance.

The lack of adequate scintillation measurements at mid latitudes led Mrak et al. (2020) to explore the use of 1-Hz data from geodetic receivers to create proxies of scintillation indices. As part of their analyses, Mrak et al. (2020) presented another unique case of moderate GPS L1 (1,575.42 MHz) scintillation, with the amplitude scintillation index S_4 (Yeh & Liu, 1982) reaching up to 0.15 on L1 as observed by a high-rate scintillation monitor deployed at The University of Texas at Dallas (UTD) in the southern US.

More recently, Rodrigues et al. (2021) showed that severe scintillations ($S_4 > 0.8$ on L2—1,227.60 MHz) can be observed by receivers in the Southern US. The observations were made on 1 June 2013 by an ionospheric scintillation and Total Electron Content (TEC) monitor also located at UTD. The study of Rodrigues et al. (2021) also indicated that the strong L-band scintillation observed over the US could be associated with extreme mid-latitude disturbances.

In this report, we present and discuss new distributed measurements made on 23–24 March 2023 by Global Navigation Satellite System (GNSS)-based scintillation monitors deployed from the magnetic equator to mid latitudes in the American sector. This new deployment of monitors target advancing our understanding about the conditions under which scintillation-causing ionospheric irregularities occur and about the severity of these scintillation events (space weather effects).

Here, we report that the distributed monitors captured an extraordinary scintillation event that extended from the magnetic equator to mid latitudes. The observed event showed unusual moderate-to-intense ionospheric L-band scintillation at mid latitudes (~40° dip latitude). The observations also show extremely intense and abnormally long-lasting (over 10 hr) L-band scintillations at low latitudes (~20° dip latitude). Additionally, the observations show the unusual occurrence of intense, post-midnight (local time) L-band scintillation at the magnetic equator. Collectively, these distributed observations captured an extraordinary scintillation event spanning a wide range of latitudes across the American sector.

Our interpretation of the 23–24 March 2023 scintillation event was assisted by maps of TEC and Rate of Change of TEC Index (ROTI), solar wind measurements, and geomagnetic indices. The TEC and ROTI maps were created as independent measurements made by distributed geodetic GNSS receivers.

Although the present report is focused on the novel observations of scintillation spanning over a wide range of latitudes and presenting abnormal severity and duration, we also show that the scintillation event of 23–24 March 2023 was associated with TEC perturbations that resemble those of EPB disturbances (EPB-like) that seem to

extend from low to mid latitudes (e.g., Aa et al., 2019; Aa et al., 2024; Chang et al., 2022; Cherniak & Zakharenkova, 2022; Martinis et al., 2015; Zakharenkova & Cherniak, 2020). While it has been noticed that these ionospheric disturbances are associated with geomagnetic disturbances, details about their generation and development are still subject of debate (e.g., Kil et al., 2016, 2024; Martinis et al., 2016).

We highlight that the lack of adequate scintillation measurements did not allow previous studies to adequately quantify the scintillation effects of these mid-latitude EPB-like events. The new distributed observations allowed us to quantify not only the spatio-temporal variation but also the severity of scintillation effects of such an event, which had yet to be done. The TEC and ROTI maps and geomagnetic information allowed us to determine the conditions leading to the spatio-temporal variation and severity of the observed scintillations.

This report is organized as follows: In Section 2, we describe the instrumentation and observations used in this study. In Section 3, we present and discuss the main results derived from observations and analyses. Finally, in Section 4, we summarize our study and main findings.

2. Instrumentation and Methodology

As mentioned earlier, scintillation observations made by monitors located at different dip latitudes in the American sector were used in this study. Maps of TEC and ROTI were also utilized to aid analyses and interpretation. Details about the instruments and measurements used in this study are provided below.

2.1. Scintillation Observations

The scintillation observations used in this report were made by ScintPi 3.0 and ScintPi 2.0 sensors (Gomez Socola & Rodrigues, 2022). ScintPi 3.0 can be described as a low-cost, easy to install and maintain GNSS-based ionospheric scintillation and TEC monitor. ScintPi 3.0 can measure amplitude scintillation in signals at two frequencies, L1 ∼ 1.6 GHz and L2 ∼ 1.2 GHz, at the rate of 20 Hz. TEC can also be estimated from ScintPi 3.0 carrier-phase and pseudo-range observables. ScintPi 2.0, on the other hand, is an even lower-cost GNSS-based, but single-frequency (L1) scintillation monitor.

These monitors have been used in studies of solar radio bursts (Wright, Solanki, et al., 2023), and studies of scintillation during geomagnetically quiet (Gomez Socola et al., 2023) and disturbed conditions (Sousasantos et al., 2023). Additionally, ScintPi has been used in educational (Wright, Rodrigues, et al., 2023) and citizen science initiatives (Sousasantos, Rodrigues, Moraes, et al., 2024).

For this study, we analyzed measurements of amplitude scintillation and TEC made on the night of 23–24 March 2023. Amplitude scintillation is quantified using the traditional amplitude scintillation index (S_4), which can be described as the standard deviation of signal amplitude normalized by the average signal amplitude in a 1-min window of data (Kintner et al., 2007).

The observations used in this study were made by ScintPi monitors deployed at 3 locations in the American sector. The locations are The University of Texas at Dallas—UTD (32.99°N, 96.76°W, 42.30° dip lat.), the Costa Rica Institute of Technology—CRT (9.85°N, 83.91°W, 19.84° dip lat.), and the Jicamarca Radio Observatory—JRO (11.95°S, 76.88°W, −0.65° dip lat.). These locations are shown in Figure 1. Only data observed within the field of view (FOV) above a 20° elevation angle was considered (dashed circles in the figure). The Ionospheric Pierce Point (IPP) was assumed at 300 km altitude for all the observations.

Dual-frequency scintillation and TEC measurements were taken at UTD and CRT using ScintPi 3.0 monitors. Single-frequency scintillation measurements were made at JRO using a ScintPi 2.0. JRO also has a ScintPi 3.0 monitor, but it was disconnected during the period of interest due to flash floods and mudslides that affected some of the JRO buildings.

2.2. ROTI and TEC Maps

To aid our interpretation of the scintillation measurements, we also used ionospheric products made available by the Institute for Space-Earth Environmental Research (ISEE) at Nagoya University (https://stdb2.isee.nagoya-u.ac.jp/GPS/GPS-TEC/). The products used in this study are the two-dimensional global maps of TEC and ROTI created using observations from more than 9,300 dual-frequency GNSS receivers. The TEC and ROTI maps are provided every 5 min in a grid resolution of 0.25° × 0.25° in geographic coordinates (latitude and longitude),

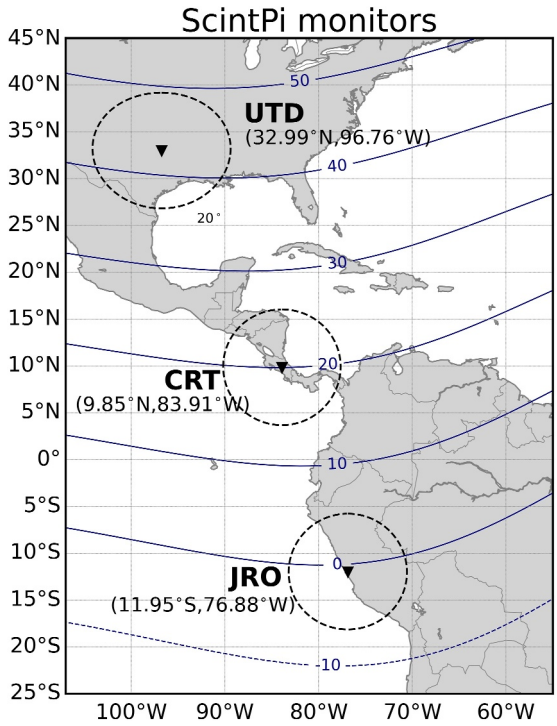

Figure 1. Map showing the location of ScintPi monitors whose measurements were used in this study. Dip latitudes computed for 300 km altitude using the International Geomagnetic Reference Field model—IGRF13 (Alken et al., 2021) are also indicated as blue isocontours. The coordinates of the stations are listed below their labels. The stations are distributed from the magnetic equator to mid latitudes in the American sector. The dashed lines indicate the 20° elevation mask considered at 300 km altitude.

assuming a thin-shell ionosphere at a height of 300 km (Sori et al., 2022). Additionally, the data provided by ISEE has been smoothed using a boxcar average of 5° × 5° grid data in geographic latitude and longitude.

ROTI values represent the standard deviation of the temporal rate of change of TEC (ΔTEC/Δt or ROT) values within an interval of 300 s. TEC samples spaced by 30 s (Δt = 30 s) were used in the computation of ROT values and, therefore, ROTI calculation used 10 ROT samples (5 min). Only data from satellites with elevation greater than 15 degrees were used in the development of the TEC and ROTI maps (Sori et al., 2022).

3. Results and Discussion

Figure 2 summarizes the scintillation observations made on 23–24 March 2023 by the UTD, CRT and JRO ScintPi monitors. It shows that the UTD monitor detected mid-latitude scintillation reaching intense levels (L1 $S_4 > 0.7$), with L1 S_4 reaching values as high as 0.8. Figure 2 also shows the occurrence of extremely intense (L1 $S_4 > 1.0$) and abnormally long-lasting scintillation in the region of transition between low and mid latitudes as observed by the CRT monitor. Furthermore, Figure 2 also shows the occurrence of intense and long-lasting scintillation at JRO, a magnetic equatorial site where L-band scintillation is typically weak and confined to pre-midnight local time hours (e.g., de Paula et al., 2003). Local midnight at Jicamarca is at 05:00 UT.

3.1. On the Occurrence of Mid-Latitude Scintillation and TEC Depletions

As previously mentioned, the observations made by the UTD monitor on 23–24 March 2023, captured a rare and unusual occurrence of mid-latitude scintillation. In the US, only a few cases of mid-latitude L-band scintillation have been reported (Ledvina et al., 2002; Mrak et al., 2020; Rodrigues et al., 2021). This is, in most part, due to the lack of adequate instrumentation for scintillation observations. The lack of observations limits our ability to identify the occurrence and severity of mid-latitude scintillation events, and the conditions under which these events develop. Moreover, previous works were not able to present simultaneous observations at different latitudes, which is important to determine the source and full impact of the underlying scintillation-inducing ionospheric disturbances. Therefore, the observations of 23–24 March 2023 presented here contribute as important experimental evidence that intense scintillation can indeed span from equatorial to mid latitudes.

Similarly to the 2013 event reported by Rodrigues et al. (2021), we found that the scintillations observed on 23–24 March 2023 were also accompanied by large-scale steep TEC depletions. This is illustrated in Figure 3 which shows examples of scintillation (S_4 increases in the upper panels for both frequencies, L1 and L2) collocated with large decreases in TEC (lower panels). The examples also illustrate that most cases of intense scintillation detected by the UTD monitor were observed on signals transmitted by satellites with low elevation angles. We address the spatio-temporal variation of scintillation observed by the monitors in the following section. The observations, nevertheless, contribute to previous studies (e.g., Erickson, 2020; Hysell et al., 2018) that point out that the mid-latitude ionosphere can be more dynamic than initially thought.

3.2. On the Spatio-Temporal Evolution of Scintillation Activity

The distributed scintillation monitors (JRO, CRT, and UTD) provide information about the latitudinal evolution of the scintillation event that was not possible in the study of Rodrigues et al. (2021), when only UTD observations were available. Additionally, the multi-GNSS capability of the monitors used in this study allows a much higher number of instantaneous observations than previously possible, which in turn provide better insight on the spatial development of scintillations within the FOV of each monitor. Only GPS measurements were available in the study of Rodrigues et al. (2021).

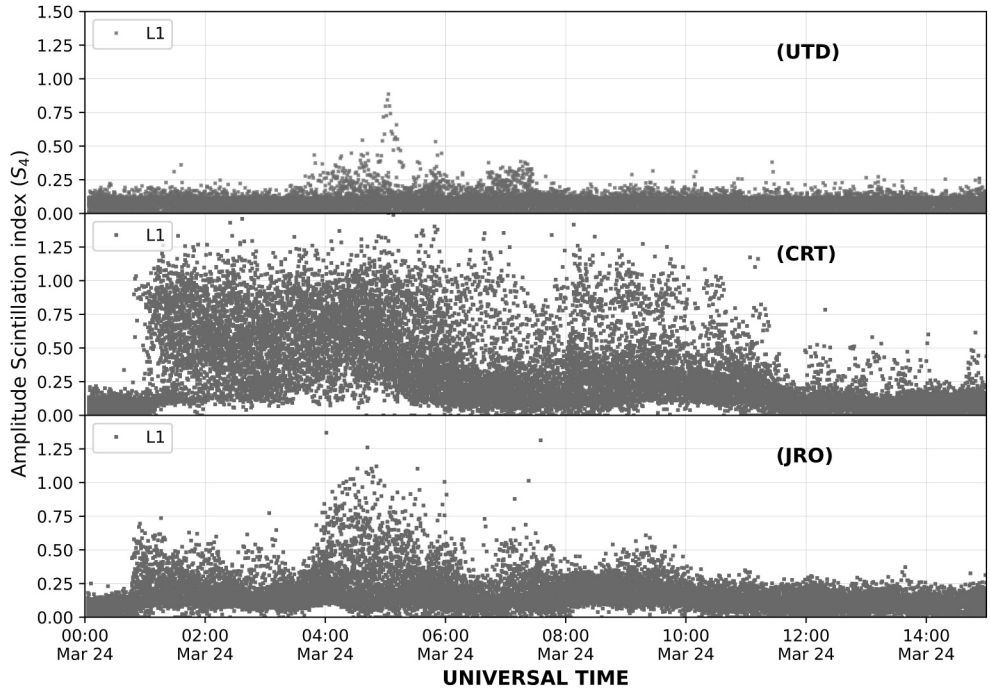

Figure 2. Values of S_4 (L1) observed by the scintillation monitors located at Jicamarca (JRO, LT ~ UT—5), Costa Rica (CRT, LT ~ UT—5.5) and at The University of Texas at Dallas (UTD, LT ~ UT—6.5). Only data from satellites with elevation angle greater than 20° are considered.

This spatio-temporal evolution of the scintillation event captured by the monitors is summarized in Figure 4. It shows the S_4 (L1) values as a function of IPP coordinates for sequential time intervals. The IPPs were computed for an ionospheric height of 300 km, the same height used in the computation of the TEC and ROTI products (see Section 2.2) that will be presented in the following sections. Note that the first 3 panels on top show observations made over 30-min intervals, while subsequent panels show observations made over 1-hr intervals.

The observations in Figure 4 show that the first cases of weak-to-moderate scintillation were observed at JRO within 00:30–01:00 UT (~19:30–20:00 LT). Local time (LT) for each monitor is computed based on monitor's universal time (UT) and longitude (UT ~ LT + Lon/15). The scintillation onset time observed is in good

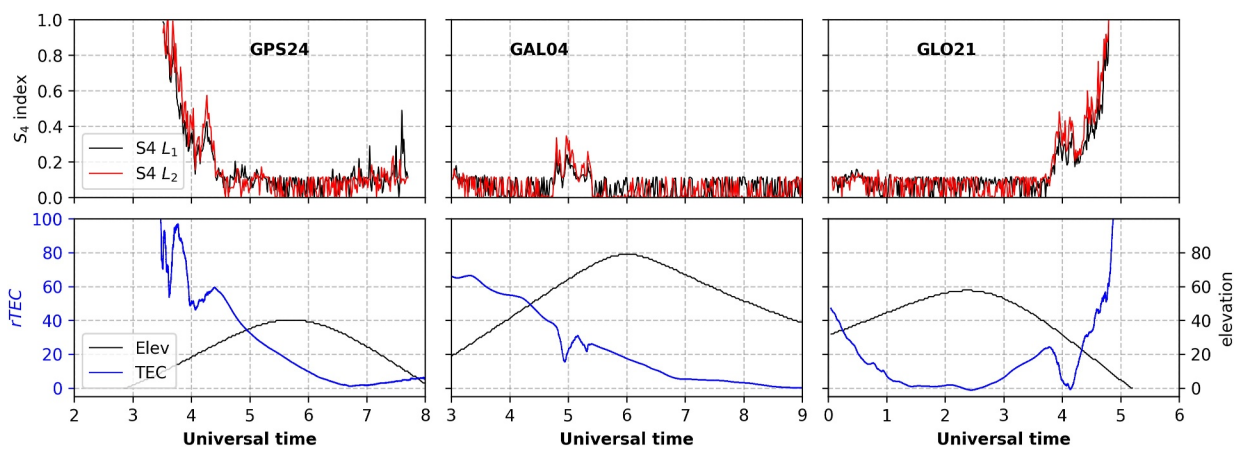

Figure 3. Examples of scintillation (upper panels) observed by the UTD monitor on 23–24 March 2023 and simultaneous slant relative TEC—rTEC (lower panels). The examples show that the observed mid-latitude scintillation was accompanied by large ionospheric irregularities (TEC depletions). TEC values are given in TEC units (TECU, 1 TECU = 1×10^{16} electrons/m^2).

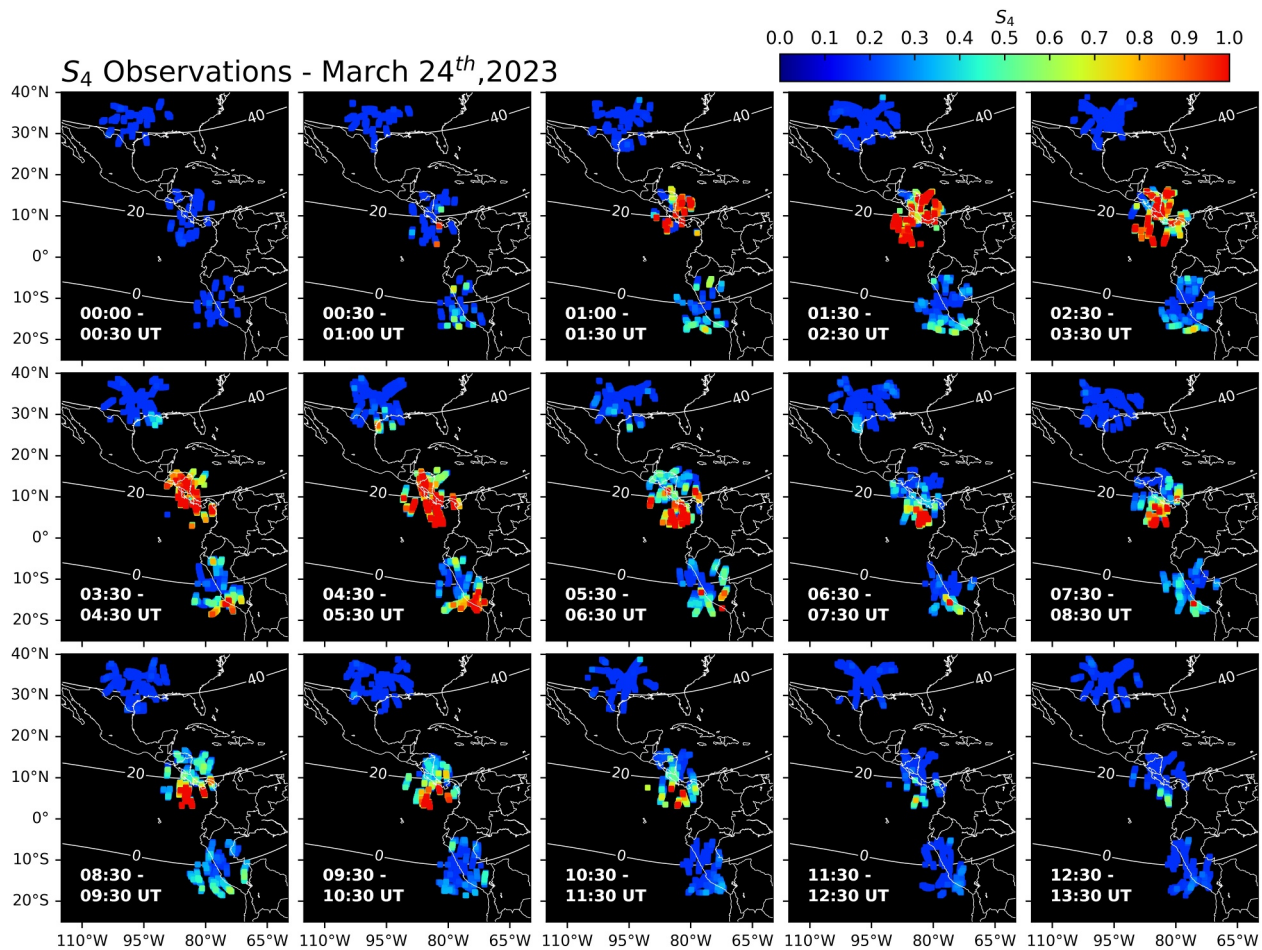

Figure 4. Spatio-temporal evolution of scintillation, S_4 (L1), over the American sector as observed by the ScintPi monitors at JRO, CRT, and UTD. The panels reveal the propagation of scintillation from low to mid latitudes and the abnormally long lasting occurrence of severe scintillation over CRT. The elevation mask of the observations is 20°.

agreement with that of ionospheric irregularities associated with post-sunset equatorial spread F (ESF) in the Peruvian sector during equinox seasons (e.g., Abdu et al., 1981; Chapagain et al., 2009).

By 01:00–01:30 UT, scintillation is detected on several IPPs observed by the JRO monitor. Figures 2 and 4 (bottom panel) also show that the JRO monitor observed intense scintillation (S_4 up to 1 or more) around local midnight (05:00 UT) followed by moderate levels of scintillation (S_4 up to ∼0.7) until about 05:00 LT (10:00 UT). We highlight that the detection of severe scintillation near the magnetic equator is highly unusual even for signals from satellites at low elevation. Near the magnetic equator, background F-region densities during post-sunset hours are reduced because of the Fountain effect (Hanson & Moffett, 1966), which cause L-band scintillation near the equator to be mostly weak (Aarons, 1982). The lack of solar photoionization reduces F-region even further during post-midnight hours.

Figure 4 does show that strong scintillation observed by the JRO monitor occurred mostly at low to moderate elevation angles (20°–60°) and to the south of the site. We hypothesize that the hemispheric asymmetry in the scintillation intensity could be associated with an asymmetry in the Equatorial Ionization Anomaly (EIA) driven, for instance, by transequatorial winds (Balan et al., 1995).

Figure 4 also shows that around 00:30–01:00 UT, a few cases of scintillation started to be detected by the CRT monitor, particularly to the south of the site. A closer inspection in the data presented in Figure 2 indicates that scintillation is observed slightly earlier at JRO compared to CRT. At 01:00–01:30 UT, however, most of the satellites observed by the CRT monitor are affected by severe scintillation.

Here, we also highlight the severity of scintillation observed by the CRT monitor. Figure 4 shows that extremely intense ($S_4 \gtrsim 1$ on L1) started to be observed by the CRT monitor around 01:30 UT and continued until 10:30–11:30 UT (05:00–06:00 LT), an abnormal total of 10 hr of extremely intense scintillation. This can perhaps better be seen in Figure 2 (middle panel).

We also point out that Figures 2 and 4 show that virtually every signal from satellites above 20° elevation observed by the CRT monitor were affected by scintillation between approximately 01:00 and 06:00 UT. Please see the elevated background S_4 values in Figure 2.

Figures 2 and 4 also show that strong scintillations are observed by the CRT monitor until around sunrise hours (11:30 UT, ∼06:00 LT). Cases of moderate and weak scintillation, however, persist well into morning hours indicating the occurrence of unusual long-lived low-latitude irregularities (e.g., Huang et al., 2013). The following section will present auxiliary, independent evidence of the occurrence of irregularities throughout the night and into the morning hours.

Around 03:30–04:30 UT scintillation starts to be observed at mid latitudes by the UTD monitor, mostly on the south portion of its FOV. Figure 4 (and Figure 2, top panel for UTD) shows that scintillation is observed by the UTD monitor between 03:30 and 07:30 UT. While no scintillation is observed by the UTD monitor after 07:30 UT, scintillation is still observed by the CRT monitor for several hours beyond this time. Here, we must emphasize again that cases of moderate scintillation observed by the CRT monitor persist until morning (∼15:00 UT, 09:30 LT), which is highly unusual and contribute to the features of this extraordinary event. See also Figure 2 (middle panel).

3.3. Ionospheric Irregularities

The spatio-temporal evolution of the scintillation observations presented in the previous section indicated that ionospheric irregularities originating at low latitudes would have created conditions favoring the development of scintillation at low-to-mid and mid latitudes. In order to confirm this hypothesis maps of ROTI covering the American sector were used.

Figure 5 presents maps of ROTI values over the American sector for the night of 23–24 March 2023 showing increased ROTI values around the times and locations where scintillations were observed. The increased ROTI values indicate the occurrence of large-scale (kilometric) TEC irregularities (Cherniak et al., 2018; Pi et al., 1997). The maps also show that, similar to scintillation, kilometric TEC irregularities persist for several hours in the American sector. Also similar to scintillation, Figure 5 shows that kilometric irregularities seem to appear first at low latitudes and then expand to mid latitudes, reaching the southern United States (∼40° dip latitude) between 03:30 UT and 04:30 UT, when scintillations were detected by the UTD monitor.

The ROTI maps also show that irregularities reaching mid latitudes are confined to a relatively narrow (in longitude) channel. Looking at the sequence of maps, particularly between 03:30 UT and 07:30 UT, it can also be noticed that this channel of irregularities is tilted to the west and shows motion in the westward direction. Note that, at 03:30 UT, elevated ROTI values at 40° dip latitude are located around 80°W. At 07:30 UT, however, elevated ROTI values at 40° dip latitude are located between 110°W and 95°W. These features are similar to those of ionospheric density depletions at mid latitudes (40°–50° dip latitudes) that started to be reported fairly recently due, in great part, to the availability of global and regional TEC maps (e.g., Aa et al., 2019, 2024; Cherniak et al., 2019; Kil et al., 2016; Martinis et al., 2015; Sori et al., 2019, 2022; Zakharenkova & Cherniak, 2020). The ROTI maps also confirm that the occurrence of ionospheric irregularities persisted beyond the sunrise, with large ROTI values seen at low latitudes until 14:30 UT (09:00 LT in Costa Rica). Additional information about the conditions favoring the extended lifetime of the observed ionospheric disturbances is provided in the following section.

The mechanism responsible for producing the TEC structures reaching mid latitudes is still a subject of discussion. Some studies have suggested that the structures are the manifestation of extreme Equatorial Plasma Bubbles (EPBs) reaching magnetic apex altitudes that map to mid latitudes (e.g., Cherniak et al., 2019; Martinis et al., 2015). Other studies suggested that these mid-latitude TEC perturbations, instead, might have been caused by Meso-Scale Traveling Ionospheric Disturbances (MSTIDs) (e.g., Kil et al., 2016). Additionally, it has also been suggested that these mid-latitude depletions are the result of a combination of processes originating at low and high latitudes (e.g., Cherniak & Zakharenkova, 2022). The mid-latitude structures would be TEC depletions

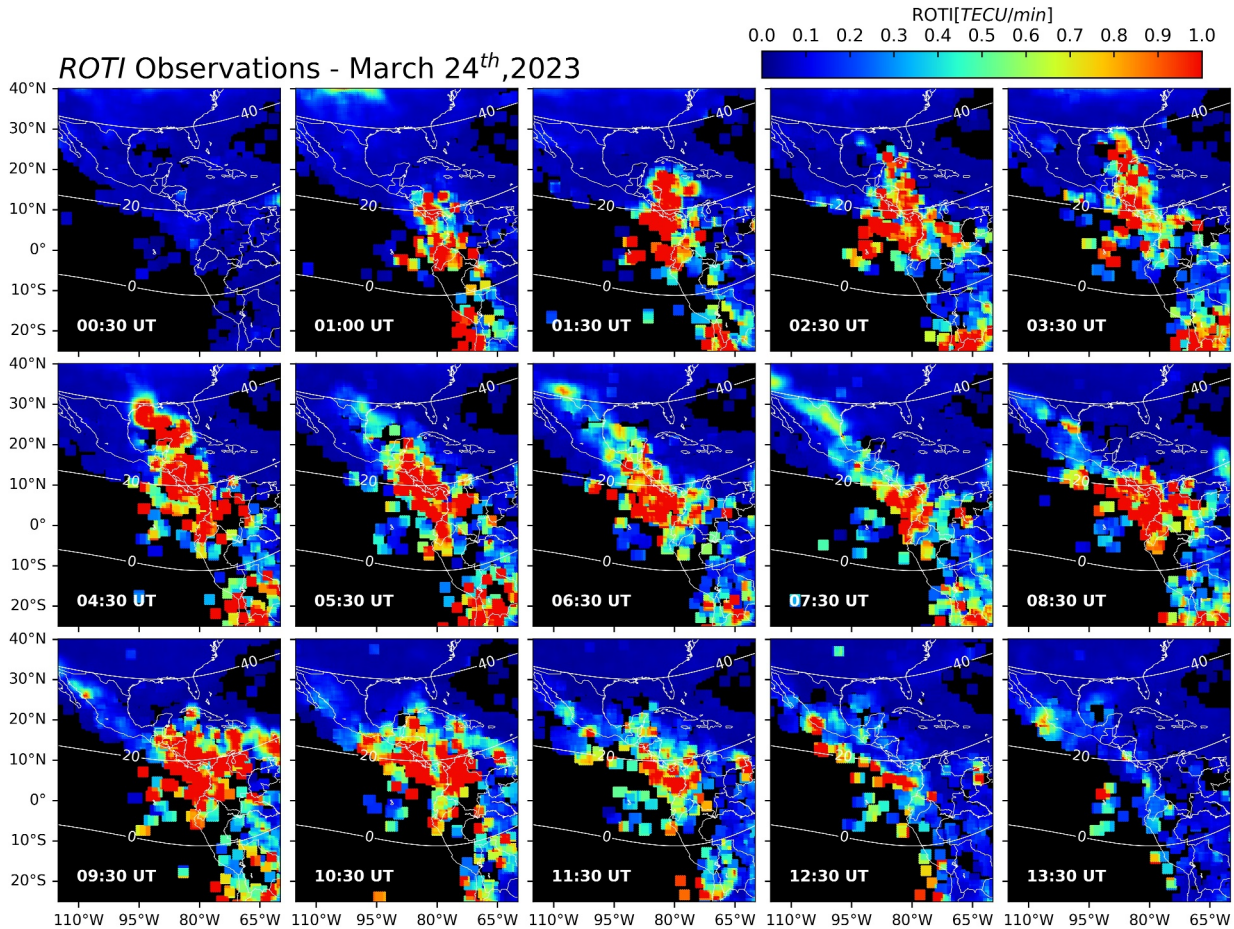

Figure 5. Snapshots of the ROTI maps for the American sector on the night of 23–24 March 2023. Isocontours of dip latitudes are indicated for reference. The ROTI maps illustrate the development of ionospheric irregularities from low to mid latitudes over time. They also show the narrow (in longitude) channel of TEC irregularities at low latitudes starting around 01:00 UT and reaching out to mid latitudes (~40° dip latitude) at 03:30 UT. ROTI values are calculated using 5 min of ROT data and are expressed in TEC units per minute (TECU/min).

originating at low latitudes as EPBs and that would then stream into mid latitudes under the action of strong subaroural electric fields (Cherniak & Zakharenkova, 2022).

While additional details and information about the relative importance of the different processes contributing to these events are subject of ongoing investigations, our study quantifies the extreme impact on GNSS signals these events can produce.

3.4. Geomagnetic Conditions

Previous studies also pointed out that EPB-like mid-latitude TEC irregularities tend to occur during geomagnetically disturbed conditions. This is another similarity on the event of 23–24 March 2023 reported here. Based on the SYM-H geomagnetic index, the extraordinary scintillation event occurred during an intense geomagnetic storm (Loewe & Prölss, 1997). Figure 6 summarizes geomagnetic conditions for 22–25 March 2023. It shows the interplanetary magnetic field component Bz, the interplanetary electric field Ey, and the SYM-H index. SYM-H shows the occurrence of a storm commencement around 04:30 UT on 23 March. Bz turned southward (i.e., $Bz < 0$) around the same time, and the main phase of the storm lasted until ~ 05:30 UT on 24 March, when SYM-H reached −170 nT and the recovery phase started. By 26 March 00:00 UT, SYM-H had not yet returned to background levels.

The scintillation event reported here occurred during the regular equatorial spread-F season in the American sector when, during geomagnetic quiet conditions, the Pre-Reversal Enhancement (PRE) of the zonal electric

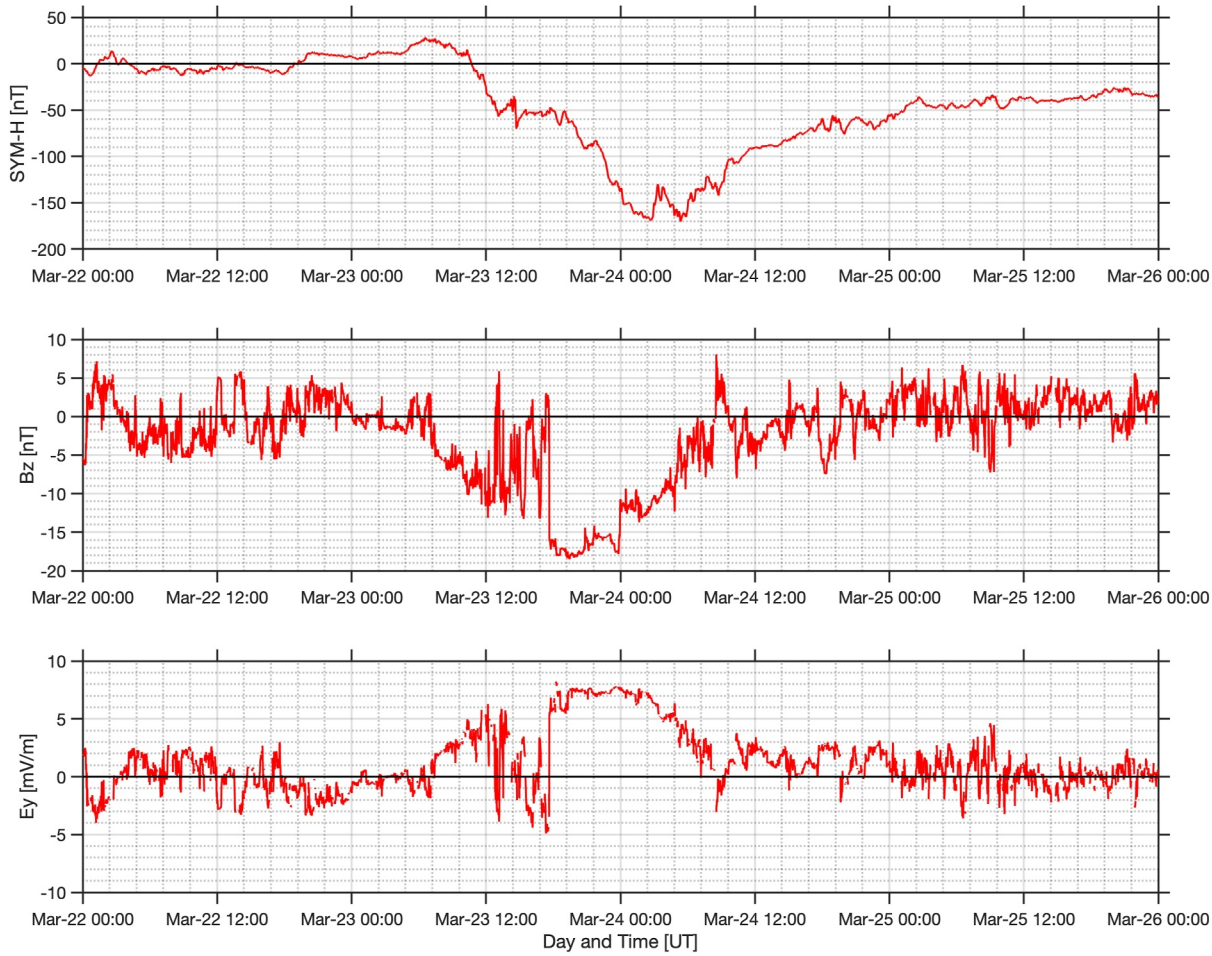

Figure 6. Information about geomagnetic conditions for 22–25 March 2023. Top, SYM-H index. Middle, Bz component of the interplanetary magnetic field. Bottom, Ey component of the interplanetary electric field.

field is pronounced (e.g., Fejer et al., 1999; Smith et al., 2016). In addition to that, Figure 6 shows substantial values of Ey (∼5 mV/m or more) between approximately 18:00 UT and 03:30 UT (∼11:00 LT and 22:30 LT for Jicamarca) indicating the possibility of prompt penetration electric fields (PPEFs) enhancing the upward equatorial F-region drifts in the American sector during afternoon and evening hours. The PPEFs could have accentuated the PRE beyond quiet-time values, creating conditions for extreme ESF and EPB development. The southward Bz conditions could have increased the efficiency of the Ey penetration (e.g., Kelley & Retterer, 2008).

An enhancement in the Auroral Electrojet (AE) index can also be seen in the quicklook plots (https://wdc.kugi.kyoto-u.ac.jp/) starting at 08:00 UT on 23 March 2023, and persisting throughout the magnetic storm. This is an indicator of geomagnetic conditions favoring the development of Disturbance Dynamo electric fields and upward drifts during post-midnight (local time) hours on 24 March. More specifically, enhancements in the AE index indicate increases in auroral currents and in Joule heating at high latitudes. The increase in Joule heating causes global thermospheric winds to depart from their regular circulation pattern. As a result, the disturbed wind dynamo can drive upward ionospheric drifts at low latitudes several hours after the AE index enhancements, particularly during local post-midnight hours (Fejer, 1991; Scherliess & Fejer, 1997).

We point out that the post-midnight upward drifts could have supported the long duration of the scintillation-causing irregularities observed at Jicamarca and Costa Rica. Our measurements do support the appearance of a new EPB during the local (American sector) post-midnight hours of the night of 23–24 March 2023. The scintillation measurements in Figure 2 show an increase in the background (minimum) S_4 values starting around 08:00 UT (∼03:00 LT) at JRO and around 08:30 UT at CRT on 24 March. Additionally, the ROTI measurements

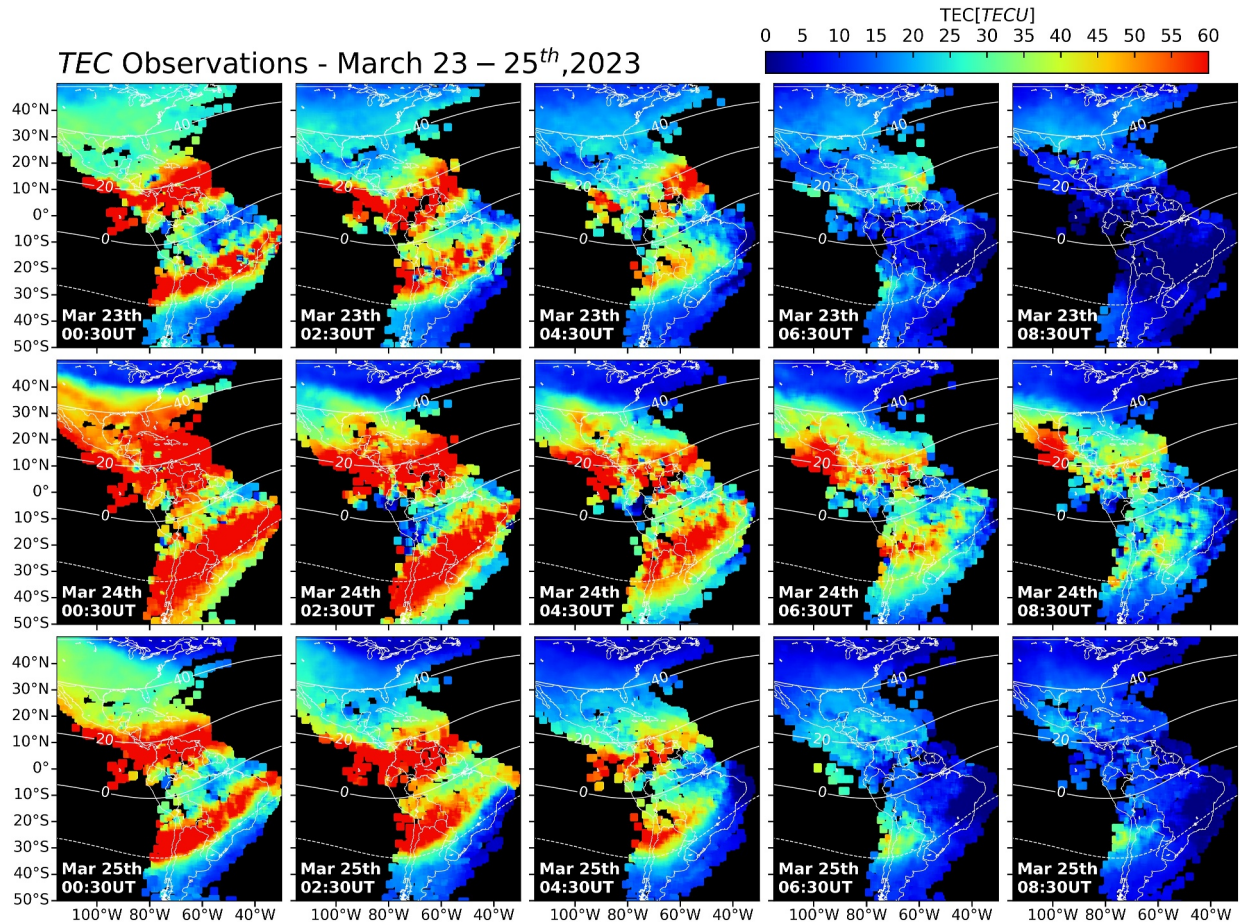

Figure 7. Snapshots of ionospheric TEC for the American sector for the three consecutive days, 23–25 March 2023. The maps serve to illustrate the enhanced TEC at low and mid latitudes on the night of 23–24 March 2023. TEC values are calculated using 5 min of data and are expressed in TEC units (TECU).

in Figure 5 also show that ionospheric structures were decaying with time until about 08:30 UT. At that time most of the increased low-latitude ROTI values were below 20° dip latitude (dip latitudes are indicated as white isocontours). At 08:30 UT, however, the ROTI values increased again in magnitude and expanded spatially at low latitudes reaching dip latitudes as high as 30°.

The development of EPBs late in the night (~08:00 UT) can explain the long-lasting occurrence of scintillation observed during this event. EPBs generated during post-midnight hours can persist until morning hours as shown by Huang et al. (2013) using in situ measurements made by sensors on the Communication/Navigation Outage Forecasting System (C/NOFS) satellite. EPBs in the morning hours would be because of the time it takes for post-midnight depletions reaching low latitudes (high altitude flux tubes) to be refilled with plasma due to the reduced recombination rates in the topside ionosphere. These long-lived EPBs would create conditions for the development of smaller scale ionospheric irregularities explaining the long-lasting scintillation event observed by the CRT monitor. L-band scintillation extending into morning hours is extremely rare, but has been reported in the past (Aarons & DasGupta, 1984).

3.5. TEC Conditions

In addition to the ROTI discussion previously presented, we now show and discuss the background TEC conditions under which ionospheric depletions, irregularities and scintillation developed. Figure 7 shows TEC maps over the American sector for 23–25 March 2023, at different UTs. It shows that the EIA was much more developed on 24 March (during the scintillation event reported here) than at the previous and following nights. TEC enhancements can be observed as far as the Southern US, consistent with the hypothesis of enhanced upward equatorial F-region drifts (and enhanced Fountain effect) during the geomagnetic storm. Besides penetration

electric fields with eastward polarity in the pre-midnight sector (local time) and disturbance dynamo electric fields in the post-midnight sector (local time), equatorward thermospheric winds at mid latitudes could also have contributed to the maintenance of the enhanced TEC observed on the night of 23–24 March.

The large background TEC levels explain the intense cases of scintillation observed by the monitors. The severity of amplitude scintillation (S_4) is controlled by the absolute density fluctuations, ΔN (Basu et al., 1976), which tend to be larger in regions of enhanced background density (de Paula et al., 2003; Sousasantos, Rodrigues, Gomez Socola, et al., 2024; Whalen, 2009). At Jicamarca, intense scintillation is observed in signals from satellites at low elevation angles (see Figure 4). In Costa Rica, intense scintillation is observed even in signals from satellites near zenith. At UTD, scintillation is observed in signals at low elevation angles and to the south. These signals traverse regions of large TEC.

We also point out that the expanded EIA during the scintillation event might have provided conditions for EPBs to reach abnormally high apex heights (and magnetic latitudes) as well. This follows the hypothesis by Mendillo et al. (2005), numerical simulations by Krall et al. (2010), and GOLD observations presented by Sousasantos et al. (2023). Mendillo et al. (2005) suggested that EPBs stop rising when the flux-tube integrated electron density inside the EPB matches the flux-tube integrated density of the surrounding background ionospheric plasma. Krall et al. (2010) showed evidence supporting the Mendillo et al. (2005) hypothesis using SAMI3/ESF numerical simulations. Using GOLD two-dimensional observations of the F-region peak density (NmF2) over the American sector, Sousasantos et al. (2023) showed a case of an EPB reaching abnormally high apex altitudes during an expanded EIA event. The expanded EIA of 23–24 March 2023 would indicate height profiles of flux-tube integrated densities with scale heights that are larger than those of geomagnetic quiet-time nights. EPBs would have to rise to higher than usual altitudes to reach a region where their internal flux-tube integrated density matches that of the background ionospheric plasma.

4. Summary of Work and Main Findings

We presented and discussed observations of an extraordinary L-band scintillation event that was detected on the night of 23–24 March 2023.

Using distributed observations, we showed that strong L-band scintillation occurred over a wide range of latitudes in the American sector, from the magnetic equator to mid latitudes (∼42° dip latitude). The distributed observations were made as the result of a new deployment of GNSS-based scintillation and TEC monitors (ScintPi) at the Jicamarca Radio Observatory (JRO, ∼−1° dip latitude) in Peru, at the Costa Rica Institute of Technology (CRT, ∼20° dip latitude) in Costa Rica, and at The University of Texas at Dallas (UTD, ∼42° dip latitude) in the US.

During this event, the JRO monitor detected intense scintillation (S_4 up to 0.7 on L1) during local pre-midnight hours and extremely intense ($S_4 \sim 1$ and above) around midnight followed by moderate scintillation (S_4 up to 0.6) in the post-midnight sector lasting until about 05:00 LT. This is a very atypical observation. L-band scintillation is known to be weak and confined to post-midnight hours near the magnetic equator due to the reduced background ionospheric F-region density. Therefore, the JRO observations indicate abnormal background density conditions around the magnetic equator during this event.

The observations made by the CRT monitor also showed extremely intense scintillations. We highlight that these extremely severe scintillations lasted for approximately 10 hr, between about 01:00 UT and 11:00 UT on 24 March. Additionally, moderate to weak scintillations were observed afterward until after sunrise, 15:00 UT (09:30 LT). This is the most intense, and long-lasting L-band scintillation event ever seen by the authors.

Observations made by the UTD monitor detected the occurrence of intense mid-latitude L-band scintillation between about 04:00 UT and 07:30 UT on 24 March. The strongest scintillation occurred around 05:00 UT with S_4 (L1) reaching values as high as 0.8. Scintillation at UTD occurred mostly to the south of the site. Here, we highlight that the detection of intense mid-latitude scintillation is extremely rare, especially in the American sector. Ledvina et al. (2002) first reported an event of intense GPS scintillation detected in the northern US. Almost 20 years later, Rodrigues et al. (2021) reported an event detected in the southern US. In both cases, observations from a single scintillation monitor only were available.

The distributed scintillation observations allowed us to obtain information that was not possible in previous studies using single site measurements. The observations allowed us to determine that scintillation-causing irregularities started near the magnetic equator and extended to mid latitudes. The observations also allowed us to determine that scintillation was accompanied by large-scale TEC depletions.

To better understand the condition under which scintillations occurred, we aided our analyses with TEC and ROTI maps produced using low-rate measurements made by distributed geodetic GNSS receivers. The ROTI maps allowed us to identify that the extraordinary scintillation event of 23–24 March was associated with an EPB-like ionospheric event reaching mid latitudes. A few examples of this type of event have been reported in previous studies, but they relied, in the most part, on TEC and ROTI maps (e.g., Aa et al., 2019, 2024; Cherniak et al., 2019; Kil et al., 2016; Martinis et al., 2015; Zakharenkova & Cherniak, 2020). Our observations contribute with unprecedented measurements of the scintillation (space weather) impact of this type of event.

Similar to cases reported in previous studies, the EPB-like disturbances associated with the 23–24 March scintillation event occurred during a major geomagnetic storm. Using interplanetary measurements and geomagnetic indices, we identified conditions favoring the occurrence of disturbance electric fields and the development of EPBs in both pre- and post-midnight sectors. The ROTI maps confirmed the development of EPBs during the pre- and post-midnight hours explaining the abnormally long duration (>10 hr) of scintillation observed at equatorial and low latitudes. EPBs generated during post-midnight hours can persist until morning hours because of the time it takes for post-midnight depletions reaching low latitudes (high altitude flux tubes) to be refilled with plasma due to the reduced recombination rates in the topside ionosphere (Huang et al., 2013).

Finally, we used the TEC maps to identify an extremely enhanced and expanded EIA during pre- and post-midnight hours of the night of 23–24 March. This provided additional evidence of the occurrence of disturbance electric fields (equatorial upward drifts) throughout the night. The enhanced background densities also explain the occurrence of strong L-band scintillation during in the post-midnight sector (Basu et al., 1976). Following the hypothesis of Mendillo et al. (2005) and numerical simulations of Krall et al. (2010), we also pointed out that the expanded EIA could have provided conditions for an EPB to reach abnormally high apex heights and magnetic latitudes.

Data Availability Statement

The ScintPi3.0 data files used in the study are publicly available at Zenodo via https://doi.org/10.5281/zenodo.13909983 (Gomez Socola & Rodrigues, 2024). Global absolute TEC and rate of the TEC index: ROTI are publicly accessible at https://stdb2.isee.nagoya-u.ac.jp/GPS/GPS-TEC/. Interplanetary Bz, Ey, and SYM_H are available at NASA/GSFC's OMNIWeb (https://omniweb.gsfc.nasa.gov).

Acknowledgments
Global GNSS-TEC data processing that produced the TEC and ROTI maps used in this study has been supported by JSPS KAKENHI Grant 16H06286. GNSS RINEX files for the GNSS-TEC processing are provided from many organizations listed by the webpage (http://stdb2.isee.nagoya-u.ac.jp/GPS/GPS-TEC/gnss_provider_list.html). We acknowledge use of NASA/GSFC's Space Physics Data Facility's OMNIWeb service, and OMNI data. FSR and JGS would like to ackowledge support from NSF through Awards AGS-2122639 and AGS-2432609. JSS would like to acknowledge support by NASA award 80NSSC24K0563.

References

Aa, E., Zhang, S. R., Zou, S., Wang, W., Wang, Z., Cai, X., et al. (2024). Significant midlatitude bubble-like ionospheric super-depletion structure (BLISS) and dynamic variation of storm-enhanced density plume during the 23 April 2023 geomagnetic storm. *Space Weather*, *22*(3), e2023SW003704. https://doi.org/10.1029/2023sw003704

Aa, E., Zou, S., Ridley, A. J., Zhang, S.-R., Coster, A. J., Erickson, P. J., et al. (2019). Merging of storm time midlatitude traveling ionospheric disturbances and equatorial plasma bubbles. *Space Weather*, *17*(2), 285–298. https://doi.org/10.1029/2018SW002101

Aarons, J. (1982). Global morphology of ionospheric scintillations. *Proceedings of the IEEE*, *70*(4), 360–378. https://doi.org/10.1109/proc.1982.12314

Aarons, J., & DasGupta, A. (1984). Equatorial scintillations during the major magnetic storm of April 1981. *Radio Science*, *19*(3), 731–739. https://doi.org/10.1029/RS019i003p00731

Abdu, M. A., Bittencourt, J. A., & Batista, I. S. (1981). Magnetic declination control of the equatorial F region dynamo electric field development and spread F. *Journal of Geophysical Research*, *86*(A13), 11443–11446. https://doi.org/10.1029/JA086iA13p11443

Alken, P., Thébault, E., Beggan, C. D., Amit, H., Aubert, J., Baerenzung, J., et al. (2021). International geomagnetic reference field: The thirteenth generation. *Earth Planets and Space*, *73*, 1–25. https://doi.org/10.1186/s40623-020-01313-z

Balan, N., Bailey, J. J., Moffett, R. J., Su, Y. Z., & Titheridge, J. E. (1995). Modeling studies of the conjugate-hemisphere differences in ionospheric ionization at equatorial anomaly latitudes. *Journal of Atmospheric and Terrestrial Physics*, *57*(3), 279–292. https://doi.org/10.1016/0021-9169(94)E0019-J

Basu, S., Basu, S., & Khan, B. K. (1976). Model of equatorial scintillations from in-situ measurements. *Radio Science*, *11*(10), 821–832. https://doi.org/10.1029/rs011i010p00821

Bevis, M., Businger, S., Chiswell, S., Herring, T. A., Anthes, R. A., Rocken, C., & Ware, R. H. (1994). GPS meteorology: Mapping zenith wet delays onto precipitable water. *Journal of Applied Meteorology*, *1988–2005*(3), 379–386. https://doi.org/10.1175/1520-0450(1994)033<0379:gmmzwd>2.0.co;2

Carrano, C. S., Groves, K. M., & Caton, R. G. (2012). Simulating the impacts of ionospheric scintillation on L band SAR image formation. *Radio Science*, *47*(4), RS0L20. https://doi.org/10.1029/2011RS004956

Chang, H., Kil, H., Sun, A. K., Zhang, S.-R., & Lee, J. (2022). Ionospheric disturbances in low- andmidlatitudes during the geomagnetic storm on 26 August 2018. *Journal of Geophysical Research: Space Physics*, *127*(2), e2021JA029879. https://doi.org/10.1029/2021JA029879

Chapagain, N. P., Fejer, B. G., & Chau, J. L. (2009). Climatology of postsunset equatorial spread F over Jicamarca. *Journal of Geophysical Research*, *114*(A7), A07307. https://doi.org/10.1029/2008JA013911

Cherniak, I., Krankowski, A., & Zakharenkova, I. (2018). ROTI maps: A new IGS ionospheric product characterizing the ionospheric irregularities occurrence. *GPS Solutions*, *22*(3), 69. https://doi.org/10.1007/s10291-018-0730-1

Cherniak, I., & Zakharenkova, I. (2022). Development of the storm-induced ionospheric irregularities at equatorial and middle latitudes during the 25–26 August 2018 geomagnetic storm. *Space Weather*, *20*(2), e2021SW002891. https://doi.org/10.1029/2021SW002891

Cherniak, I., Zakharenkova, I., & Sokolovsky, S. (2019). Multi-instrumental observation of storm-induced ionospheric plasma bubbles at equatorial and middle latitudes. *Journal of Geophysical Research: Space Physics*, *124*(3), 1491–1508. https://doi.org/10.1029/2018JA026309

de Paula, E. R., Rodrigues, F. S., Iyer, K. N., Kantor, I. J., Abdu, M. A., Kintner, P. M., et al. (2003). Equatorial anomaly effects on GPS scintillations in Brazil. *Advances in Space Research*, *31*(3), 749–754. https://doi.org/10.1016/S0273-1177(03)00048-6

de Paula, E. R. D., Monico, J. F. G., Tsuchiya, Í. H., Valladares, C. E., Costa, S. M. A., Marini-Pereira, L., et al. (2023). A retrospective of global navigation satellite system ionospheric irregularities monitoring networks in Brazil. *Journal of Aerospace Technology and Management*, *15*, e0123. https://doi.org/10.1590/jatm.v15.1288

Erickson, P. E. (2020). *Mid-latitude ionospheric features: Natural complexity in action, chapter in the dynamic ionosphere* (pp. 25–38). Elsevier.

Fejer, B. G. (1991). Low latitude electrodynamic plasma drifts: A review. *Journal of Atmospheric and Terrestrial Physics*, *53*(8), 677–693. https://doi.org/10.1016/0021-9169(91)90121-M

Fejer, B. G., Scherliess, L., & De Paula, E. R. (1999). Effects of the vertical plasma drift velocity on the generation and evolution of equatorial spread F. *Journal of Geophysical Research*, *104*(A9), 19859–19869. https://doi.org/10.1029/1999ja900271

Gomez Socola, J., & Rodrigues, F. (2024). Data sets for distributed ionospheric L-band scintillation and TEC observations made in the American sector during the 23–24 March 2023 geomagnetic storm [Dataset]. *Zenodo*. https://doi.org/10.5281/zenodo.13909983

Gomez Socola, J., & Rodrigues, F. S. (2022). ScintPi 2.0 and 3.0: Low-cost GNSS-based monitors of ionospheric scintillation and total electron content. *Earth Planets and Space*, *74*(1), 185. https://doi.org/10.1186/s40623-022-01743-x

Gomez Socola, J., Sousasantos, J., Rodrigues, F. S., Brum, C. G. M., Terra, P., Moraes, A. O., & Eastes, R. (2023). On the quiet-time occurrence rates, severity and origin of L-band ionospheric scintillations observed from low-to-mid latitude sites located in Puerto Rico. *Journal of Atmospheric and Solar-Terrestrial Physics*, *250*, 106123. https://doi.org/10.1016/j.jastp.2023.106123

Groves, K. M., Basu, S., Weber, E. J., Smitham, M., Kuenzler, H., Valladares, C. E., et al. (1997). Equatorial scintillation and systems support. *Radio Science*, *32*(5), 2047–2064. https://doi.org/10.1029/97rs00836

Hanson, W. B., & Moffett, R. J. (1966). Lonization transport effects in the equatorial F region. *Journal of Geophysical Research*, *71*(23), 5559–5572. https://doi.org/10.1029/JZ071i023p05559

Huang, C.-S., de La Beaujardiere, O., Roddy, P. A., Hunton, D. E., Ballenthin, J. O., & Hairston, M. R. (2013). Long-lasting daytime equatorial plasma bubbles observed by the C/NOFS satellite. *Journal of Geophysical Research: Space Physics*, *118*(5), 2398–2408. https://doi.org/10.1002/jgra.50252

Hysell, D., Larsen, M., Fritts, D., Laughman, B., & Sulzer, M. (2018). Major upwelling and overturning in the mid-latitude F region ionosphere. *Nature Communications*, *9*(1), 3326. https://doi.org/10.1038/s41467-018-05809-x

Jayachandran, P. T., Langley, R. B., MacDougall, J. W., Mushini, S. C., Pokhotelov, D., Hamza, A. M., et al. (2009). Canadian high arctic ionospheric network (CHAIN). *Radio Science*, *44*(1), 1–10. https://doi.org/10.1029/2008rs004046

Jiao, Y., & Morton, Y. T. (2015). Comparison of the effect of high-latitude and equatorial ionospheric scintillation on GPS signals during the maximum of solar cycle 24. *Radio Science*, *50*(9), 886–903. https://doi.org/10.1002/2015rs005719

Kelley, M. C., & Retterer, J. (2008). First successful prediction of a convective equatorial ionospheric storm using solar wind parameters. *Space Weather*, *6*(8), S08003. https://doi.org/10.1029/2007SW000381

Kelly, M. A., Comberiate, J. M., Miller, E. S., & Paxton, L. J. (2014). Progress toward forecasting of space weather effects on UHF SATCOM after Operation Anaconda. *Space Weather*, *12*(10), 601–611. https://doi.org/10.1002/2014SW001081

Kil, H., Miller, E. S., Jee, G., Kwak, Y.-S., Zhang, Y., & Nishioka, M. (2016). Comment on "The night when the aur- oral and equatorial ionospheres con-verged" by Martinis, C. J. Baumgardner, M. Mendillo, J. Wroten, A. Coster, and L. Paxton. *Journal of Geophysical Research: Space Physics*, *121*(10), 10599–10607. https://doi.org/10.1002/2016JA022662

Kil, H., Sun, A. K., Lee, W. K., Chang, H., & Lee, J. (2024). Assessment of the origin of a plasma depletion band over the United States during the 8 September 2017 geomagnetic storm. *Geophysical Research Letters*, *51*(7), e2024GL108334. https://doi.org/10.1029/2024GL108334

Kintner, P. M., Ledvina, B. M., & De Paula, E. R. (2007). GPS and ionospheric scintillations. *Space Weather*, *5*(9), S09003. https://doi.org/10.1029/2006SW000260

Krall, J., Huba, J. D., Ossakow, S. L., & Joyce, G. (2010). Why do equatorial ionospheric bubbles stop rising? *Geophysical Research Letters*, *37*(9), 1–4. https://doi.org/10.1029/2010GL043128

Ledvina, B. M., Makela, J. J., & Kintner, P. M. (2002). First observations of intense GPS L1 amplitude scintillations at midlatitude. *Geophysical Research Letters*, *29*(14). https://doi.org/10.1029/2002GL014770

Liu, Y.-H., Liu, C.-H., & Su, S.-Y. (2012). Global and seasonal scintillation morphology in the equatorial region derived from ROCSAT-1 in-situ data. *Terrestrial, Atmospheric and Oceanic Sciences*, *23*(1), 95–106. https://doi.org/10.3319/TAO.2011.06.30.01(AA)

Loewe, C. A., & Prölss, G. W. (1997). Classification and mean behavior of magnetic storms. *Journal of Geophysical Research*, *102*(A7), 14209–14213. https://doi.org/10.1029/96JA04020

Luo, X., Chen, Z., Gu, S., Yue, N., & Yue, T. (2023). Studying the fixing rate of GPS PPP ambiguity resolution under different geomagnetic storm intensities. *Space Weather*, *21*(10), e2023SW003542. https://doi.org/10.1029/2023sw003542

Martinis, C., Baumgardner, J., Mendillo, M., Wroten, J., Coster, A., & Paxton, L. (2015). The night when the auroral and equatorial ionospheres converged. *Journal of Geophysical Research: Space Physics*, *120*(9), 8085–8095. https://doi.org/10.1002/2015JA021555

Martinis, C., Baumgardner, J., Mendillo, M., Wroten, J., Coster, A. J., & Paxton, L. J. (2016). Reply to comment by Kil et al. on "The night when the auroral and equatorial ionospheres converged". *Journal of Geophysical Research: Space Physics*, *121*(10), 10–608. https://doi.org/10.1002/2016ja022914

McGranaghan, R. M., Mannucci, A. J., Wilson, B., Mattmann, C. A., & Chadwick, R. (2018). New capabilities for prediction of high-latitude ionospheric scintillation: A novel approach with machine learning. *Space Weather*, *16*(11), 1817–1846. https://doi.org/10.1029/2018sw002018

Mendillo, M., Zesta, E., Shodhan, S., Sultan, P. J., Doe, R., Sahai, Y., & Baumgardner, J. (2005). Observations and modeling of the coupled latitude-altitude patterns of equatorial plasma depletions. *Journal of Geophysical Research*, *110*(A9303), 1–7. https://doi.org/10.1029/2005JA011157

Monico, J. F. G., Camargo, P. O., Alves, D. B. M., Shimabukuro, M. H., Aquino, M., Pereira, V. A. S., & Vani, B. C. (2013). From CIGALA to CALIBRA: An infrastructure for ionospheric scintillation monitoring in Brazil. In *AGU meeting of Americas in Cancun*.

Monico, J. F. G., Paula, E. R. D., Moraes, A. D. O., Costa, E., Shimabukuro, M. H., Alves, D. B. M., et al. (2022). The GNSS NavAer INCT project overview and main results. *Journal of Aerospace Technology and Management*, *14*, e0722. https://doi.org/10.1590/jatm.v14.1249

Moraes, A., Sousasantos, J., Costa, E., Pereira, B. A., Rodrigues, F., & Galera Monico, J. F. (2024). Characterization of scintillation events with basis on L1 transmissions from geostationary SBAS satellites. *Space Weather*, *22*(1), e2023SW003656. https://doi.org/10.1029/2023SW003656

Mrak, S., Semeter, J., Nishimura, Y., Rodrigues, F. S., Coster, A. J., & Groves, K. (2020). Leveraging geodetic GPS receivers for ionospheric scintillation science. *Radio Science*, *55*(11), e2020RS007131. https://doi.org/10.1029/2020RS007131

Pi, X., Mannucci, A. J., Lindqwister, U. J., & Ho, C. M. (1997). Monitoring of global ionospheric irregularities using the worldwide GPS network. *Geophysical Research Letters*, *24*(18), 2283–2286. https://doi.org/10.1029/97gl02273

Redmon, R. J., Anderson, D., Caton, R., & Bullett, T. (2010). A forecasting ionospheric real-time scintillation tool (FIRST). *Space Weather*, *8*(12). https://doi.org/10.1029/2010sw000582

Rodrigues, F. S., Socola, J. G., Moraes, A. O., Martinis, C., & Hickey, D. A. (2021). On the properties of and ionospheric conditions associated with a mid-latitude scintillation event observed over southern United States. *Space Weather*, *19*(6), e2021SW002744. https://doi.org/10.1029/2021SW002744

Scherliess, L., & Fejer, B. G. (1997). Storm time dependence of equatorial disturbance dynamo zonal electric fields. *Journal of Geophysical Research*, *102*(A11), 24037–24046. https://doi.org/10.1029/97JA02165

Smith, J. M., Rodrigues, F. S., Fejer, B. G., & Milla, M. A. (2016). Coherent and incoherent scatter radar study of the climatology and day-to-day variability of mean F region vertical drifts and equatorial spread F. *Journal of Geophysical Research: Space Physics*, *121*(2), 1466–1482. https://doi.org/10.1002/2015JA021934

Sori, T., Otsuka, Y., Shinbori, A., Nishioka, M., & Perwitasari, S. (2022). Geomagnetic conjugacy of plasma bubbles extending to mid-latitudes during a geomagnetic storm on March 1, 2013. *Earth Planets and Space*, *74*(1), 120. https://doi.org/10.1186/s40623-022-01682-7

Sori, T., Shinbori, A., Otsuka, Y., Tsugawa, T., & Mishioka, M. (2019). Characteristics of GNSS total electron content enhancements over the midlatitudes during a geomagnetic storm on 7 and 8 November 2004. *Journal of Geophysical Research: Space Physics*, *124*(12), 10376–10394. https://doi.org/10.1029/2019JA026713

Sousasantos, J., Gomez Socola, J., Rodrigues, F. S., Eastes, R. W., Christiano, C. M. B., & Terra, P. (2023). Severe L-band scintillation over low-to-mid latitudes caused by an extreme equatorial plasma bubble: Joint observations from ground-based monitors and GOLD. *Earth Planets and Space*, *75*(1), 41. https://doi.org/10.1186/s40623-023-01797-5

Sousasantos, J., Marini-Pereira, L., Moraes, A., & Pullen, S. (2021). Ground-based augmentation system operation in low latitudes -Part 2: Space weather, ionospheric behavior and challenges. *Journal of Aerospace Technology and Management*, *13*. https://doi.org/10.1590/jatm.v13.1237

Sousasantos, J., Rodrigues, F. S., Gomez Socola, J., Pérez, C., Colvero, F., Martinis, C. R., & Wrasse, C. M. (2024). First observations of severe scintillation over low-to-mid latitudes driven by quiet-time extreme equatorial plasma bubbles: Conjugate measurements enabled by citizen science initiatives. *Journal of Geophysical Research: Space Physics*, *129*(6), e2024JA032545. https://doi.org/10.1029/2024JA032545

Sousasantos, J., Rodrigues, F. S., Moraes, A. O., Eastes, R. W., & Monico, J. F. G. (2024). On the estimation of scintillation severity using background F-region peak densities: Description and example results using GOLD observations. *GPS Solutions*, *28*(2), 62. https://doi.org/10.1007/s10291-023-01602-6

Valladares, C. E., & Chau, J. L. (2012). The low-latitude ionosphere sensor network: Initial results. *Radio Science*, *47*(4), 1–18. https://doi.org/10.1029/2011rs004978

Veettil, S. V., Aquino, M., Spogli, L., & Cesaroni, C. (2018). A statistical approach to estimate Global Navigation Satellite Systems (GNSS) receiver signal tracking performance in the presence of ionospheric scintillation. *Journal of Space Weather and Space Climate*, *8*, A51. https://doi.org/10.1051/swsc/2018037

Whalen, J. A. (2009). The linear dependence of GHz scintillation on electron density observed in the equatorial anomaly. *Annals of Geophysics*, *27*(4), 1755–1761. https://doi.org/10.5194/angeo-27-1755-2009

Wright, I. G., Rodrigues, F. S., Gomez Socola, J., Moraes, A. O., Monico, J. F. G., Sojka, J., et al. (2023). On the detection of a solar radio burst event that occurred on 28 August 2022 and its effect on GNSS signals as observed by ionospheric scintillation monitors distributed over the American sector. *Journal of Space Weather and Space Climate*, *13*, 28. https://doi.org/10.1051/swsc/2023027

Wright, I. G., Solanki, I., Desai, A., Socola, J. G., & Rodrigues, F. S. (2023). Student-led design, development and tests of an autonomous, low-cost platform for distributed space weather observations. *Journal of Space Weather and Space Climate*, *13*, 12. https://doi.org/10.1051/swsc/2023010

Yeh, K. C., & Liu, C. H. (1982). Radio wave scintillations in the ionosphere. *Proceedings of the IEEE*, *70*(4), 324–360. https://doi.org/10.1109/PROC.1982.12313

Zakharenkova, I., & Cherniak, I. (2020). When plasma streams tie up equatorial plasma irregularities with auroral ones. *Space Weather*, *18*(2), e2019SW002375. https://doi.org/10.1029/2019sw002375

Zakharenkova, I., & Cherniak, I. (2021). Effects of storm-induced equatorial plasma bubbles on GPS-based kinematic positioning at equatorial and middle latitudes during the September 7–8, 2017, geomagnetic storm. *GPS Solutions*, *25*(4), 132. https://doi.org/10.1007/s10291-021-01166-3